ResearchGate

See discussions, stats, and author profiles for this publication at:
https://www.researchgate.net/publication/269466183

Extant ionic charge theory for bond orbital model based on the tight-binding method: A semi-empirical model applied to wide-band gap II–VI and III–V semiconductors

ARTICLE *in* MATERIALS SCIENCE IN SEMICONDUCTOR PROCESSING · JANUARY 2015

Impact Factor: 1.96 · DOI: 10.1016/j.mssp.2014.05.033

READS

83

1 AUTHOR:

A. S. Verma

Banasthali University

73 PUBLICATIONS **474** CITATIONS

SEE PROFILE

All in-text references underlined in blue are linked to publications on ResearchGate, letting you access and read them immediately.

Available from: A. S. Verma
Retrieved on: 27 January 2016

Materials Science in Semiconductor Processing 29 (2015) 2–15

Contents lists available at ScienceDirect

Materials Science in Semiconductor Processing

journal homepage: www.elsevier.com/locate/mssp

Review

Extant ionic charge theory for bond orbital model based on the tight-binding method: A semi-empirical model applied to wide-bandgap II-VI and III-V semiconductors

A.S. Verma *

Department of Physics, Banasthali Vidyapith, Rajasthan 304022, India

ARTICLE INFO

Available online 6 June 2014

PACS:
D83
62.20.de
62.20M-
61.82Fk

Keywords:
Semiconductors
Elastic properties
Mechanical properties

ABSTRACT

In order to enhance the viability of this review for that issue, I suggest adding this to the beginning of the Abstract: "Binary semiconductors with II-VI and III-V composition, owing to their direct and typically rather wide gap, are technologically important materials. The recent successful fabrication of the blue-green laser diode based on these compounds has renewed interest in their physical properties In this review the correlations are presented for the bond polarity (α_p), hybrid covalent energy (V_2) and elastic constants (C_{ij}) and may be represented by linear equations. These are simple function of product of ionic charges of cation and anion (Z_1Z_2) and nearest neighbour distance (d in Å). On the basis of this result a bond orbital calculations based on the tight-binding method is used to estimate the hybrid covalency (α_c), hybrid polar energy (V_3), effective charge, transverse effective charge (e_T), Kleinman's internal displacement parameter (ζ), bulk modulus (B), shear constant $(C_{11}-C_{12})/2$, shear modulus (G), Young's modulus (Y), bond stretching force constants (α), bond bending force constants (β) of a number of ordered A^NB^{8-N} semiconductors. The proposed expressions can be applied to a broad selection of covalent materials and their predictions are in good agreement with the experimental data and those from ab initio calculations.

© 2014 Elsevier Ltd. All rights reserved.

Contents

1. Introduction

$A^{III}B^{V}$ and $A^{II}B^{VI}$ semiconductors, owing to their direct and rather large gap, are technologically important materials. The recent successful fabrication of the blue-green

* Mobile: +91 9412884655.
E-mail address: ajay_phy@rediffmail.com

http://dx.doi.org/10.1016/j.mssp.2014.05.033
1369-8001/© 2014 Elsevier Ltd. All rights reserved.

laser diode based on these compounds has renewed interest in their physical properties. These materials are characterized by different degrees of covalent, ionic, and metallic bonding, and they crystallize in different crystal structures such as zinc blende and wurtzite. The common and dominant feature of these structures is the tetrahedral bonding to four atoms of the other elements. In zinc blende these tetrahedral are arranged in a cubic type structure whilst they are in a hexagonal type structure. Indeed, the centres of similar tetrahedral are arranged in a face-centered cubic (*fcc*) array in the former and a hexagonal closed-packed (*hcp*) array in the latter [1]. The particular omnitriangulated nature in atomic structure gives these materials unique physical properties.

The elastic properties of materials are of considerable importance in determining the residual stress state in thin film structures after processing and for optimizing growth conditions in multilayers. The elastic moduli of the compounds are of importance in assessing the competition between the ductile and brittle failures. These have been extensively investigated in relation to various microscopic characteristic of different sorts of materials, such as metals and covalently bonded crystals. The comparison of the properties of different tetrahedral semiconductors becomes fundamental; when dealing with the study and characterization of complex semiconductor systems with mixed composition (e.g., superlattices, semiconductor alloys). Some tools such as Raman spectroscopy have been shown to be very efficient from the experimental point of view. Within this context, the investigation of the growth properties of new materials often requires the analysis of the elastic behaviour of the constituents, in connexion with the response to hydrostatic or uniaxial stresses. In the past decades, numerous efforts for the elastic properties of semiconductors have been made by many researchers, using, for example, semiempirical model [2,3], a bond-orbital model (BOM) [4,5], a first-principles linear-combination of the atomic orbitals method [6,7], pseudopotential methods with the LDA and GGA [8–10], the linear muffin–tin orbitals method [11], the universal tight-binding parameters method [12], and the extended Huckel tight-binding method [13]. Recent developments in modeling, through the use of density functional theory and the increased availability of computational power, have made predictions of elastic properties ab initio from theoretical principles relatively straightforward. However, one has to keep in mind that the rationalization of these first principles calculations often requires profound understanding of the nature of the chemical bonding and its attributes in various solid systems.

Because these calculations are complex and required significant effort, empirical calculations [14,15], have been developed to compute properties of zinc blende solids. The empirical relations have become widely recognized as the method of choice for computational solid-state studies. Empirical concepts such as ionic charge, empirical radii, electronegativity, ionicity and plasmon energy are then useful [16,17]. These concepts are directly associated with the character of the chemical bond and thus provide means for explaining and classifying many basic properties of molecules and solids. Very recently, the author [18–23] studied the properties of binary and ternary compounds with the help of ionic charge theory of solids. This is due to the fact that the ionic charge depends on the number of valence electrons, which changes when a metal forms a compound.

In order to obtain the structural trends, the simple ionic charge theory is used to study the elastic properties of semiconductors systematically. We have calculated the elastic constants (C_{11} and C_{12}), bond polarity (α_p), elastic stiffness constant (C_{44}), hybrid covalency (α_c), hybrid covalent energy (V_2), hybrid polar energy (V_3), effective charge, transverse effective charge (e_T), Kleinman's internal displacement parameter (ζ), bulk modulus (B), shear constant $(C_{11}-C_{12})/2$, shear modulus (G), Young's modulus (Y), bond stretching force constants (α), bond bending force constants (β) for zinc blende semiconductors and compare the values with others from theoretical calculations and experiments.

2. Tight binding theory

The tight-binding theory evolved into an essentially first-principles theory and took such a simple form that it provides a clear way to think about all of the trends from system to system entirely in terms of concepts which arise within the simple formalism. The total energy expressed in terms of local orbitals, however, has required extensive computation for ionic and covalent solids [5,24,25]. In spite of the important progress in tight-binding calculations of equilibrium spacing, cohesive energy and force constants for the rocksalt and zinc blende structure solids [24]; it is still difficult to calculate the equilibrium spacing for all semiconductors in good accordance with experiment. In particular, the fact that the lattice spacing of all the zinc blende structure compounds formed from elements in the same row of the periodic table is nearly the same is still a puzzle. In tetrahedrally coordinated solids four orthogonal and normalized sp^3 hybrids are chosen in which the electron charge density is the greatest in the direction of the nearest neighbours.

A hybrid $|\alpha\rangle$ on a cation atom and $|\beta\rangle$ on a neighbouring anion form by a linear combination,

$$|\Psi\rangle = U_\alpha|\alpha\rangle + U_\beta|\beta\rangle \tag{1}$$

the bonding and antibonding states. The U_α and U_β are constant coefficients which for bonding and antibonding combinations can be expressed by the bond polarity [5]. The one-electron Hamiltonian of the system is approximated by the kinetic energy and the sum of free-atom potentials for the cation and anion atoms. It has been shown that the one-electron average energy, which is the bond energy can be approximated by the following expression [5,24]:

$$\varepsilon_b = \frac{1}{2}(\varepsilon_h^\alpha + \varepsilon_h^\beta) - (V_2^2 + V_3^2)^{1/2} + SV_2 \tag{2}$$

The first term is the average of the cation and anion hybrid energy where for sp^3 bonds:

$$\varepsilon_h^\alpha = \frac{1}{4}(\varepsilon_s^\alpha + 3\varepsilon_p^\alpha), \quad \varepsilon_h^\beta = \frac{1}{4}(\varepsilon_s^\beta + 3\varepsilon_p^\beta) \tag{3}$$

and ε_s^α, ε_p^α, ε_s^β and ε_s^β are the free-atom energies for s and p states for the cation anion respectively.

The second term is connected with the σ-type bond formation energy and V_2, the hybrid covalent energy, and V_3, the hybrid ionic energy, which can be approximated in the following way:

$$V_2 = -\frac{\eta_\sigma \hbar^2}{md^2} \tag{4}$$

where

$$\eta_\sigma = \frac{1}{4}\eta_{ss\sigma} - \left(\frac{2\sqrt{3}}{4}\right)\eta_{sp\sigma} - \frac{3}{4}\eta_{pp\sigma}$$
$$V_3 = \frac{1}{2}(\varepsilon_h^\alpha - \varepsilon_h^\beta) \tag{5}$$

where d is the nearest neighbour distance and $\eta_{ss\sigma} = -1.40$, $\eta_{sp\sigma} = 1.84$ and $\eta_{pp\sigma} = 3.24$ are dimensionless Harrison universal parameters (Harrison). This term is responsible for the lowering of the energy due to the σ-type bond formation.

The third term is identified with the overlap interactions and is responsible for the forces which prevent the collapse of matter under the attractive σ bonding energy. The hybrids considered are orthogonal only when they are on the same atomic site. However, hybrids on adjacent sites are not orthogonal and they have non-zero overlap, $S = \langle\alpha|\beta\rangle$.

In the extended Huckel theory of quantum chemistry the following approximation is used (Hoffmann):

$$V_2 = k|\overline{\varepsilon_h}|S \tag{6}$$

where $\overline{\varepsilon_h}$ is a cation–anion average hybrid energy, and k is an empirical parameter.

The arithmetic average of cation and anion hybrid energy has previously been used to obtain $\overline{\varepsilon_h}$ [24]. However for tetrahedral ionic solids it seems more appropriate to take the following weighted average:

$$\overline{\varepsilon_h} = \frac{1}{8}(n_c\varepsilon_h^c + n_a\varepsilon_h^a) \tag{7}$$

where n_c and n_a are the number of electrons associated with the cation and anion respectively, which participate in the bonds ($n_c = 1, 2, 3$ and $n_a = 7, 6, 5$) for $A^{I}B^{VII}$, $A^{II}B^{VI}$ and $A^{III}B^{V}$ compounds respectively. The definition of the average hybrid energy given by Eq. (7) is the only new factor which drastically improves the tight-binding approach to bond theory. In the approximations adopted here the covalent interaction $V_2 \sim 1/d^2$ [26].

Within this approximation, the equilibrium spacing is obtained by taking the derivative of Eq. (2) with respect to d and setting it to zero

$$\frac{\partial E_b}{\partial d} = 4\frac{V_2^2}{\sqrt{V_2^2+V_3^2}} - 8V_2S = 0 \tag{8}$$

The value of S at the equilibrium spacing is

$$S = \frac{1}{2}\frac{V_2}{\sqrt{V_2^2+V_3^2}} = \frac{1}{2}\alpha_C \tag{9a}$$

where α_c is called the hybrid covalency and also defined by

$$\alpha_c = \sqrt{1-\alpha_p^2} \quad (\alpha_p \text{ is hybrid polarity}) \tag{9b}$$

An effective charge (Z_{eff}) for the cation can be obtained in tight binding theory as the column number (it is less than four for a cation) for that element minus the sum over occupied states of the squared amplitudes of the orbitals of that atom. The anion has a nuclear charge of $(4+\Delta Z)e$, where $4+\Delta Z$ is the column number in the Periodic Table. $\Delta Z = 0$ for carbon, 1 for nitrogen, 2 for oxygen, and 3 for fluorine. The bond orbital approximation gives an approximate value of [5]

$$Z_{eff} = 4\alpha_p - \Delta Z \tag{9c}$$

In all cases the electron transfer is in the direction of the motion of the anion. Thus the dynamic charge adds to the effective charge in Eq. (9c) to give a macroscopic transverse effective charge of

$$e_T = 4\alpha_p - \Delta Z + 4\gamma\alpha_p(1-\alpha_p^2) \tag{9d}$$

where γ is a parameter which would be unity if the hybrids were non-overlapping and spherically symmetric and if there were no local field effects. Harrison [5] has used $\gamma^2 = 2$ to give an appropriate scale, and we will use in our calculations. The fact that it is larger than one suggests that as a bond becomes polar the principal charge transfer is between the far sides of the corresponding ions.

The hybrid polarity of the compound can be obtained from,

$$\alpha_p = \frac{V_3}{\sqrt{V_2^2+V_3^2}} \tag{10a}$$

After solving Eqs. (10a) and (9b), Eq. (5) for hybrid ionic energy (V_3) may be extended by the following relation:

$$V_3 = \frac{V_2\alpha_c}{\alpha_p} \tag{10b}$$

According to the bond orbital method proposed by Baranowski [26], the bulk modulus is given by

$$B = \frac{2\sqrt{3}}{3}\left(V_2\alpha_C^3 + \frac{7.8}{d^2}\right)\frac{1}{d^3} \tag{11}$$

where α_c, V_2 and d are hybrid covalency, hybrid covalent energy and bond length respectively. The elastic shear constant $(C_{11}-C_{12})/2$ is given by

$$\frac{(C_{11}-C_{12})}{2} = \frac{\sqrt{3}}{4}\left(V_2\alpha_C^3(1+\lambda) - \frac{3}{4}|V_{pp\pi}|\right)\frac{1}{d^3} \tag{12}$$

where λ is a dimensionless parameter, which is defined as follows;

$$\lambda = \frac{\sqrt{3}V_{sp\sigma} - 3V_{pp\sigma}}{V_{ss\sigma} - 2\sqrt{3}V_{sp\sigma} - 3V_{pp\sigma}} \tag{13}$$

where $Vsp\sigma$, $Vpp\sigma$, $Vss\sigma$ and $Vpp\pi$ in Eq. (12) are the matrix elements [5], combining Eqs. (11) and (12) and $B = \frac{1}{2}(C_{11}+2C_{12})$, one can obtain the following elastic constants:

$$C_{11} = \frac{\sqrt{3}}{3}\left(V_2\alpha_C^3(3+\lambda) - \frac{3}{4}|V_{pp\pi}| + 2\frac{7.8}{d^2}\right)\frac{1}{d^3} \tag{14}$$

and

$$C_{12} = \frac{\sqrt{3}}{6}\left(V_2\alpha_C^3(3-\lambda) + \frac{3}{4}|V_{pp\pi}| + 4\frac{7.8}{d^2}\right)\frac{1}{d^3} \tag{15}$$

within the framework of the valence force field model [5], the elastic stiffness constant C_{44} of zinc blende structure semiconductors is given by

$$C_{44}=\frac{3(C_{11}+2C_{12})(C_{11}-C_{12})}{(7C_{11}+2C_{12})} \tag{16}$$

The macroscopic elastic constants B and $(C_{11}-C_{12})/2$ are related to the inter atomic force constants α and β by Eq. [27],

$$3B=\frac{\sqrt{3}}{4d}(3\alpha+\beta)-0.355SC_0 \tag{17}$$

and

$$\frac{(C_{11}-C_{12})}{2}=\frac{\sqrt{3}}{2d}\beta-0.053SC_0 \tag{18}$$

here SC_0 is the Coulomb contribution (rather small for all zinc blende structure semiconductors). If we neglect the Coulomb contribution, the bond stretching force constant α and bond bending force constant β may be obtained from [28],

$$\alpha=\frac{4d}{\sqrt{3}}B-\frac{1}{3}\beta \tag{19}$$

$$\beta=\frac{d(C_{11}-C_{12})}{\sqrt{3}} \tag{20}$$

According to the BOM proposed by Harrison [5], the elastic shear constant $(C_{11}-C_{12})/2$ is given as

$$\frac{(C_{11}-C_{12})}{2}=\frac{\sqrt{3}\lambda V_2\alpha_c^3}{2d^3} \tag{21}$$

According to Eqs. (18) and (21)

$$\frac{(C_{11}-C_{12})}{2}=\frac{\sqrt{3}\lambda V_2\alpha_c^3}{2d^3}=\frac{\sqrt{3}}{2d}\beta \times(\text{after neglecting Coulomb contribution}) \tag{22}$$

$$\beta=\frac{\lambda V_2\alpha_c^3}{d^2} \tag{23}$$

Kitamura et al. have defined that the bulk modulus may be given as

$$B=\frac{\lambda V_2}{d^3} \tag{24}$$

According to Eqs. (19), (23) and (24) bond stretching force constant may be given as

$$\alpha=\frac{4d}{\sqrt{3}}B-\frac{1}{3}\beta=\frac{\lambda V_2}{d^2}\left(\frac{4}{\sqrt{3}}-\frac{\alpha_c^3}{3}\right) \tag{25}$$

3. Concept of ionic charge theory

A chemical bond is formed when the atoms with incomplete valence shells combine. There are following main types of bonds:

1. Ionic or electrovalent bond.
2. Covalent bond.
3. Coordinate bond.
4. Metallic bond.

The valence electrons refer to the electrons that take part in chemical bonding. These electrons reside in the outer most electron shell of the atom. The participation of valence shell electrons in chemical bonding may be explained on the basis of following grounds:

(i) The outermost-shell electrons are farthest away form the nucleus and therefore, are not very firmly bound to the nucleus.
(ii) The outermost-shell electrons of an atom are also close to any foreign atom that may approach them and are therefore the first to be attracted by the approaching atom.

The author in the previous research [18–20] found that substantially reduced ionic charges must be used to get better agreement with experimental values. In the extended Huckel theory of quantum chemistry hybrid covalent energy V_2 depends on the cation–anion average hybrid energy ($\overline{\varepsilon_h}$); which is directly related to number of electrons associated with the cation and anion. Ionic charge depends on the outermost-shell electrons of an atom. Thus, there must be a correlation between ionic charge and the properties of solids.

4. Verification of ionic charge theory from the graphs and proposed expressions for elastic properties

As an example to verification of ionic charge theory, we have plotted a curve between experimental C_{11} and $1/d^3$ for $A^{III}B^{V}$ and $A^{II}B^{VI}$ semiconductors and presented in Fig. 1. We observe that in the plot of C_{11} and nearest neighbour distance (d in Å); the groups $A^{III}B^{V}$ and $A^{II}B^{VI}$ semiconductors lie on two different lines. This effect induced by the ionic charges of the compounds in the case of $A^{III}B^{V}$ and $A^{II}B^{VI}$ semiconductors. If all experimental data of C_{11} plots with product of ionic charges (Z_1Z_2) and nearest neighbour distance (d in Å) of $A^{III}B^{V}$ and $A^{II}B^{VI}$ semiconductors and

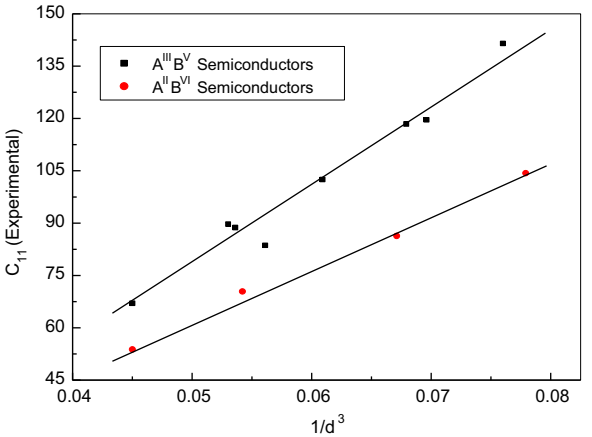

Fig. 1. Plot of C_{11} (10^{11} erg/cm^3) and $1/d^3$ (nearest neighbour distance in Å) for the group $A^{II}B^{VI}$ and group $A^{III}B^{V}$, the group $A^{II}B^{VI}$ lie on line nearly parallel to the line for group $A^{III}B^{V}$, which is depending upon the product of ionic charges. In this figure elastic constant values are taken from experimental data.

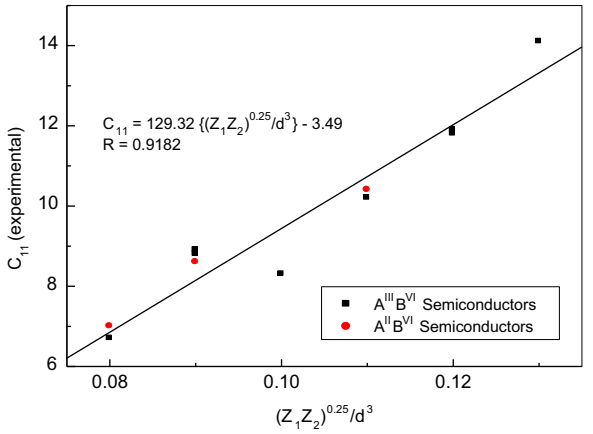

Fig. 2. Plot of C_{11} (10^{11} erg/cm^3) and $(Z_1Z_2)^{0.25}/d^3$ (nearest neighbour distance in Å) for the group $A^{II}B^{VI}$ and group $A^{III}B^{V}$. In this figure elastic constant values are taken from experimental data.

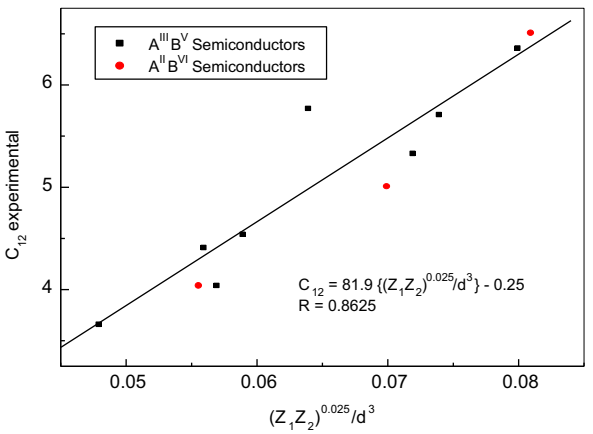

Fig. 3. Plot of C_{12} (10^{11} erg/cm^3) and $(Z_1Z_2)^{0.025}/d^3$ (nearest neighbour distance in Å) for the group $A^{II}B^{VI}$ and group $A^{III}B^{V}$. In this figure elastic constant values are taken from experimental data.

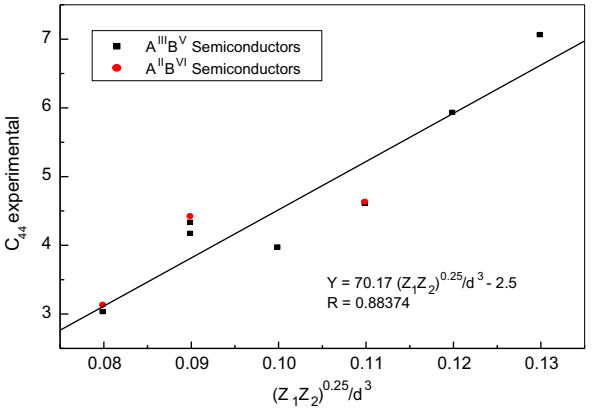

Fig. 4. Plot of C_{44} (10^{11} erg/cm^3) and $(Z_1Z_2)^{0.25}/d^3$ (nearest neighbour distance in Å) for the group $A^{II}B^{VI}$ and group $A^{III}B^{V}$. In this figure elastic constant values are taken from experimental data.

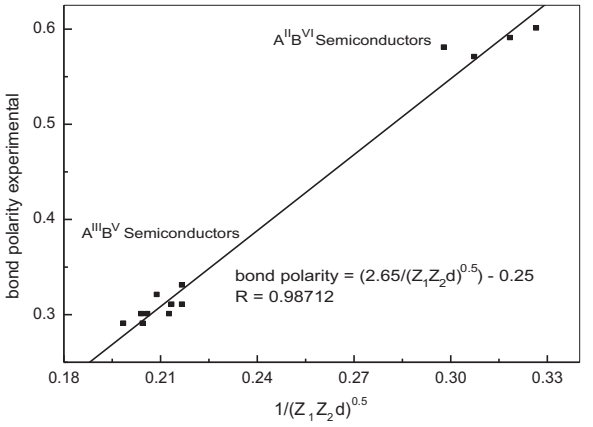

Fig. 5. Plot of α_p and $1/\sqrt{(Z_1Z_2d)}$ (nearest neighbour distance in Å) for the group $A^{II}B^{VI}$ and group $A^{III}B^{V}$. In this figure polarity values are taken from experimental data [28].

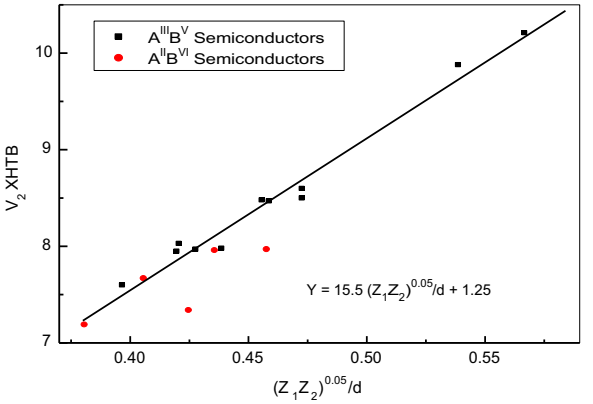

Fig. 6. Plot of V_2 XHTB and $(Z_1Z_2)^{0.05}/d$ (nearest neighbour distance in Å) for the group $A^{II}B^{VI}$ and group $A^{III}B^{V}$. In this figure V_2 data are taken from Ref. [13].

found a straight line for both groups, which are presented in Fig. 2. If we compare between Figs. 1 and 2 and found that two lines in Fig. 1 due to different ionic charges of the compounds. The above condition has been found for all parameters (C_{12}, C_{44}, α_p and V_2). In this review, we have presented only main figures, which have been plotted for linear regression lines. In Figs. 2–6, it has been verified that elastic moduli assume a decreasing linear trend with increasing nearest neighbour distance (d in Å). Therefore, based on Eqs. (5) and (6) the fact that V_2, α_p, C_{11}, C_{12} and C_{44} are linear functions of ionic charge and increasing nearest neighbour distance (d in Å). These elastic moduli are expected to exhibit the following explicit dependences on d and (Z_1Z_2):

$$V_2 = 1.25 + 15.5\left(\frac{(Z_1Z_2)^{0.05}}{d}\right) \quad (R = 0.978) \tag{26}$$

$$\alpha_p = -0.25 + 2.65\left(\frac{1}{\sqrt{Z_1Z_2d}}\right) \quad (R = 0.987) \tag{27}$$

$$C_{ij} = \delta_{ij} + \gamma_{ij}\left(\frac{(Z_1 Z_2)^{\mu_{ij}}}{d^3}\right) \quad (28)$$

The constants δ_{ij}, γ_{ij} and μ_{ij}, are given in Table 1 with the correlation coefficient (R) obtained from the regression analysis. It is clear from Figs. 2–6 and table (A) that Eqs. (26)–(28) describe well the behaviour of all V_2, α_p, C_{11}, C_{12} and C_{44} values and that the correlation is appropriate.

It is noteworthy that in most cases, the reported ab initio values of bulk and shear modulus were extrapolated from the elastic constants through the following relations [2]:

$$B = \frac{(C_{11} + 2C_{12})}{3} \quad (29)$$

$$G = \frac{(C_{11} - C_{12} + C_{44})}{5} \quad (30)$$

Table 1
Values of constants.

Elastic modulus	δ_{ij}	γ_{ij}	μ_{ij}	R
C_{11} (10^{11} ergs/cm^3)	−3.49	129.32	0.25	0.9182
C_{12} (10^{11} ergs/cm^3)	−0.25	81.9	0.025	0.8626
C_{44} (10^{11} ergs/cm^3)	−2.50	70.17	0.25	0.8837

Table 2
Results for hybrid covalent energy (V_2 in eV) from the Eq. (26) and band structure calculations based on the Bond Orbital Method (BOM) and Extended Huckel Tight Binding (XHTB).

Solids	d (Å)	λ	V_2 XHTB [13]	V_2 BOM [13]	V_2 (this work)
BN	1.57	0.728[b]	11.50	9.96	12.27
BP	1.97	0.771[b]	10.20	6.33	10.03
BAs	2.07	0.773[b]	9.87	5.73	9.61
BSb	2.24	0.800[a]			8.97
AlN	1.87	0.730[a]			10.50
AlP	2.36	0.779[b]	8.49	4.41	8.58
AlAs	2.43	0.784[b]	8.46	4.16	8.37
AlSb	2.66	0.802[b]	7.94	3.47	7.75
GaN	1.88	0.731[a]			10.45
GaP	2.36	0.779[b]	8.59	4.41	8.58
GaAs	2.45	0.786[b]	8.47	4.09	8.31
GaSb	2.65	0.803[b]	8.02	3.50	7.78
InN	2.08	0.732[a]			9.57
InP	2.54	0.781[b]	7.97	3.81	8.06
InAs	2.61	0.786[b]	7.96	3.61	7.88
InSb	2.81	0.804[b]	7.59	3.11	7.41
TiN	2.11	0.734[a]			9.45
TiP	2.49	0.782[a]			8.20
TiAs	2.58	0.785[a]			7.96
TiSb	2.75	0.803[a]			7.54
ZnS	2.34	0.737[b]	7.96	4.49	8.35
ZnSe	2.46	0.753[b]	7.95	4.09	8.00
ZnTe	2.64	0.779[b]	7.66	3.52	7.54
CdS	2.52	0.735[b]	7.33	3.84	7.84
CdSe	2.62	0.754[a]			7.59
CdTe	2.81	0.776[b]	7.18	3.11	7.16
HgS	2.53	0.736[a]			7.82
HgSe	2.63	0.755[a]			7.57
HgTe	2.8	0.777[a]			7.18
BeS	2.1	0.757[b]	9.16	5.57	9.16
BeSe	2.2	0.765[b]	9.11	5.07	8.80
BeTe	2.4	0.785[b]	8.58	4.26	8.17

[a] Calculated.
[b] Ref. [13].

Young's modulus is a measure of the stiffness of a given material. It describes tensile elasticity or the tendency of a material to deform along an axis when opposing forces are applied along that axis. The knowledge of Young's modulus is useful for the prediction of compression of an object. The obtained elastic constants C_{11} and C_{12} allowed us also to calculate the Young's modulus (Y) using the following relation [29]:

$$Y = \frac{(C_{11} + 2C_{12})(C_{11} - C_{12})}{(C_{11} + C_{12})} \quad (31)$$

Within the framework of the valence force field model, the Kleinman's internal displacement parameter (ζ) of diamond and zinc blende structure semiconductors is given by [5],

$$\zeta = \frac{C_{11} + 8C_{12}}{7C_{11} + 2C_{12}} \quad (32)$$

5. Results and discussion

We have presented the results for the hybrid covalency (α_c), hybrid polar energy (V_3), effective charge, transverse

Table 3
Results for polarity (α_p) obtained from Eq. (27) and band structure calculations based on the Bond Orbital Method (BOM), Huckel Tight Binding (HTB), Extended Huckel Tight Binding (XHTB), Phillips (Ph), cluster method (cl), Brillouin-zone (BZ) integration of the LCAO Hamiltonian. These values are listed in Ref. [28].

Solids	α_p								
	Ph	cl	BZ	UTBP	HTB	XHTB	BOM	Exp	This work
BN									0.45
BP									0.38
BAs									0.36
BSb									0.34
TiN									0.36
TiP									0.31
TiAs									0.30
TiSb									0.28
AlN									0.40
AlP		0.42	0.44				0.34	0.33	0.33
AlAs		0.39	0.41				0.34	0.31	0.32
AlSb		0.32	0.34				0.29	0.3	0.29
GaN									0.39
GaP	0.57	0.38	0.4	0.35	0.42	0.59	0.48	0.31	0.33
GaAs	0.56	0.35	0.37	0.33	0.37	0.53	0.47	0.3	0.31
GaSb	0.51	0.28	0.3	0.27	0.26	0.38	0.39	0.29	0.29
InN									0.36
InP	0.65	0.46	0.48	0.43	0.46	0.66	0.58	0.32	0.30
InAs	0.6	0.42	0.44	0.4	0.42	0.61	0.56	0.3	0.30
InSb	0.57	0.35	0.37	0.35	0.33	0.49	0.5	0.29	0.28
ZnS	0.79	0.55	0.56	0.61	0.62	0.86	0.73	0.6	0.62
ZnSe	0.79	0.55	0.56	0.6	0.58	0.82	0.73	0.59	0.59
ZnTe	0.77	0.54	0.55	0.57	0.51	0.73	0.7	0.57	0.57
CdS									0.58
CdSe									0.57
CdTe	0.82	0.58	0.59	0.63	0.54	0.77	0.75	0.58	0.54
HgS									0.58
HgSe									0.57
HgTe									0.54
BeS									0.66
BeSe									0.64
BeTe									0.61

effective charge (e_T), Kleinman's internal displacement parameter (ζ), bulk modulus (B), shear constant $(C_{11}-C_{12})/2$, shear modulus (G), Young's modulus (Y), bond stretching force constants (α), bond bending force constants (β). New correlations are presented for the bond polarity (α_p), hybrid covalent energy (V_2) and elastic

Table 4
Values of hybrid covalency (α_c) defined by Eq. (9b) and of effective charge (Z_{eff}) defined by Eq. (9c) obtained for zinc blende solids by using the Modified Tight Binding (MTB) method. The values of hybrid covalency and effective charge are tabulated as Bond Orbital Method (BOM), Extended Huckel Tight Binding (XHTB), Phillips (PHIL), experimental (exp) for comparison from Refs. [13,28].

Solids	α_c				Z_{eff}			
	XHTB	PHIL	BOM	This work	XHTB	BOM	Exp	This work
BN	0.725	0.862	0.974	0.891	1.75	−0.096	0.55	0.82
BP	0.977	0.971	0.991	0.925	−0.158	−0.452		0.52
Bas	0.993	0.987	0.992	0.931	−0.533	−0.48		0.46
BSb				0.940				0.36
TiN				0.934				0.43
TiP				0.951				0.24
TiAs				0.954				0.20
TiSb				0.959				0.13
AlN				0.918				0.58
AlP	0.777	0.782	0.942	0.946	1.51	0.35	0.30	0.30
AlAs	0.819	0.754	0.941	0.949	1.3	0.35	0.26	0.27
AlSb	0.905	0.753	0.957	0.957	0.7	0.16	0.19	0.17
GaN				0.919				0.58
GaP	0.808	0.82	0.947	0.946	1.35	0.28	0.24	0.30
GaAs	0.849	0.831	0.948	0.949	1.12	0.27	0.20	0.26
GaSb	0.924	0.86	0.965	0.956	0.53	0.05	0.15	0.17
InN				0.932				0.45
InP	0.752	0.761	0.918	0.953	1.64	0.59	0.27	0.22
InAs	0.791	0.801	0.917	0.955	1.45	0.59	0.21	0.19
InSb	0.875	0.82	0.937	0.961	0.94	0.38	0.16	0.11
ZnS	0.517	0.614	0.836	0.788	1.42	0.2	0.42	0.46
ZnSe	0.574	0.614	0.833	0.804	1.28	0.21	0.34	0.38
ZnTe	0.679	0.633	0.84	0.825	0.94	0.17	0.28	0.26
CdS	0.488	0.567	0.789	0.811	1.49	0.46		0.34
CdSe				0.823				0.27
CdTe	0.636	0.569	0.792	0.841	1.09	0.44	0.32	0.16
HgS				0.812				0.33
HgSe				0.824				0.27
HgTe				0.840				0.17
BeS	0.611	0.845	0.922	0.747	1.17	−0.451		0.66
BeSe	0.672	0.86	0.922	0.766	0.96	−0.452		0.57
BeTe	0.792	0.912	0.928	0.796	0.44	−0.511		0.42

Table 6
Results for the values of hybrid ionic energy (V_3 in eV) defined by Eq. (10b), and the value of $\lambda V_2/d^3$ in 10^{11} ergs/cm^3 obtained for the zinc blende solids using the Modified Tight Binding (MTB) method. For comparison, the values of $\lambda V_2/d^3$ obtained from BOM, XHTB and the experimental bulk modulus (exp) are also tabulated in units of 10^{11} ergs/cm^3.

Solids	d (Å)	V_2 (this work)	V_3 [26]	$V_2\alpha_p/\alpha_c$	$\lambda V_2/d^3$			
				V_3 (this work)	BOM	XHTB	Exp	This work
BN	1.57	12.27	3.15	6.27	35.2	34.6	36.9	36.9
BP	1.97	10.03	1.20	4.11	11.3	16.5	17.2	16.2
BAs	2.07	9.61	1.07	3.75	8.8	13.8		13.4
BSb	2.24	8.97		3.25				10.2
AlN	1.87	10.50	4.09	4.53				18.8
AlP	2.36	8.58	2.17	2.95	4.58	8.1	8.6	8.1
AlAs	2.43	8.37	2.04	2.79	3.96	7.4	7.7	7.3
AlSb	2.66	7.75	1.48	2.36	2.52	5.4	5.9	5.3
GaN	1.88	10.45	3.92	4.48				18.4
GaP	2.36	8.58	2.00	2.95	4.58	8.2	8.87	8.2
GaAs	2.45	8.31	1.87	2.75	3.8	7.2	7.48	7.1
GaSb	2.65	7.78	1.30	2.38	2.57	5.5	5.6	5.4
InN	2.08	9.57	4.15	3.72				12.5
InP	2.54	8.06	2.23	2.57	3.18	6.1	7.25	6.2
InAs	2.61	7.88	2.10	2.45	2.77	5.6	5.8	5.6
InSb	2.81	7.41	1.54	2.13	1.92	4.4	4.66	4.3
TiN	2.11	9.45		3.62				11.7
TiP	2.49	8.20		2.67				6.6
TiAs	2.58	7.96		2.50				5.8
TiSb	2.75	7.54		2.22				4.7
ZnS	2.34	8.35	4.13	6.53	4.79	7.3	7.8	7.7
ZnSe	2.46	8.00	3.8	5.92	3.8	6.5	5.95	6.5
ZnTe	2.64	7.54	3.04	5.17	2.61	5.2	5.1	5.1
CdS	2.52	7.84	4.22	5.65	3.24	5.3	6.4	5.8
CdSe	2.62	7.59	3.88	5.25				5.1
CdTe	2.81	7.16	3.13	4.60	1.92	4	4.2	4.0
HgS	2.53	7.82	4.18	5.61				5.7
HgSe	2.63	7.57	3.85	5.21				5.0
HgTe	2.8	7.18	3.09	4.63				4.1
BeS	2.1	9.16		8.14	8.22	12		12.0
BeSe	2.2	8.80		7.40	6.51	10.5		10.1
BeTe	2.4	8.17		6.21	4.21	7.8		7.4

Table 5
Values of transverse effective charge (e_T^*) defined by Eq. (9d) obtained for zinc blende solids by using the Modified Tight Binding (MTB) method. The values of transverse effective charge (e_T^*) are tabulated as Bond Orbital Method (BOM) and Experimental (Exp) for comparison from Ref. [28].

Solids	α_p (this work)	BOM [28]	Exp [28]	e_T^* (this work)	Solids	α_p (this work)	BOM [28]	Exp [28]	e_T^* (this work)
BN	0.455	0.476	2.47	2.86	InN	0.362			2.23
BP	0.379	−0.93		2.35	InP	0.304	1.48	2.55	1.78
BAs	0.364	−0.139		2.24	InAs	0.297	1.49	2.53	1.72
BSb	0.340			2.06	InSb	0.277	1.19	2.42	1.55
TiN	0.358			2.20	ZnS	0.616	1.22	2.15	2.63
TiP	0.310			1.82	ZnSe	0.595	1.23	2.03	2.55
TiAs	0.300			1.74	ZnTe	0.565	1.19	2	2.44
TiSb	0.283			1.60	CdS	0.585	1.48	2.77	2.52
AlN	0.396			2.47	CdSe	0.569			2.45
AlP	0.325	1.15	2.28	1.94	CdTe	0.540	1.46	2.35	2.33
AlAs	0.317	1.15	2.3	1.88	HgS	0.583			2.51
AlSb	0.292	0.864	1.93	1.68	HgSe	0.567			2.44
GaN	0.394			2.46	HgTe	0.542			2.33
GaP	0.325	1.04	2.04	1.94	BeS	0.664	0.427		2.76
GaAs	0.314	1.03	2.16	1.86	BeSe	0.643	0.426		2.71
GaSb	0.293	0.703	2.15	1.68	BeTe	0.605	0.344		2.59

Table 7
Values of the elastic constants (C_{11}, C_{12} and C_{44}) in 10^{11} ergs/cm^3 defined by Eq. (28) and of Kleinman's internal displacement parameter (ζ) defined by Eq. (32) obtained for zinc blende solids. The values of shear constants $(C_{11}-C_{12})/2$ in 10^{11} ergs/cm^3 are also tabulated together with experimental and theoretical values reported by previous researchers.

Solids	C_{11}	C_{12}	C_{44}	$(C_{11}-C_{12})/2$	ζ Eq. (32)	Method	Ref.
AlN	30.8	13	16.1	8.9	0.56	This work	
	29.6	15.7	20	6.95	0.65	PW-PP	[9]
	32.8	13.9	13.3	9.45	0.56	LSF	[37]
	34.8	16.8	13.5	9	0.61	Ab initio	[31]
	29.8	16.4	18.7	6.7	0.67	DFT	[1]
AlP	13.6	6.3	6.8	3.65	0.59	This work	
	13.3	6.7	6.3	3.3	0.63	PW-PP	[9]
	12.9	5.6	5.2	3.65	0.57	XHTB	[34]
	13.4	6.8	7	3.3	0.63	DFT	[1]
AlAs	12.1	5.8	6	3.15	0.61	This work	
	12	5.8	5.7	3.1	0.61	Exp	[33]
	12.4	4.9	5.1	3.75	0.53	XHTB	[34]
	12.9	5.5	5.2	3.7	0.56	BOM	[33]
	11.6	5.5	5.7	3.05	0.60	Ab initio	[33]
	11.3	5.6	5.5	2.85	0.62	PW-PP	[9]
AlSb	8.4	4.4	4	2	0.64	This work	
	8.9	4.4	4.2	2.25	0.62	Exp	[9]
	9.8	3.2	4.3	3.3	0.47	XHTB	[34]
	9.2	3.9	3.7	2.65	0.56	BOM	[33]
	8.6	4.1	4	2.25	0.61	PW-PP	[9]
GaN	30.2	12.8	15.8	8.7	0.56	This work	
	31.7	15.2	19.8	8.25	0.61	PW-PP	[9]
	28.5	16.1	14.9	6.2	0.68	DFT	[1]
	29.3	15.9	15.5	6.7	0.66	Ab initio	[32]
	26.4	15.3	6.8	5.55	0.69	LSF	[37]
GaP	13.6	6.3	6.8	3.65	0.59	This work	
	14.1	6.3	7.1	3.9	0.58	Exp	[9]
	13.5	5.5	5.6	4	0.55	XHTB	[34]
	14.5	6.2	5.9	4.15	0.56	BOM	[33]
	14.7	6.1	7.9	4.3	0.55	Ab initio	[33]
	15.1	6.3	7.6	4.4	0.55	PW-PP	[9]
	14.7	6.1	7.9	4.3	0.55	DFT	[1]
GaAs	11.7	5.6	5.8	3.05	0.61	This work	
	11.8	5.3	5.9	3.25	0.58	Exp	[9]
	12.5	4.6	5.3	3.95	0.51	XHTB	[34]
	12.5	5.3	5.1	3.6	0.56	BOM	[33]
	12.3	5.3	6.2	3.5	0.57	Ab initio	[33]
	12.4	5.1	6.3	3.65	0.55	PW-PP	[9]
	12.1	5.5	6.7	3.3	0.59	DFT	[1]
GaSb	8.6	4.4	4	2.1	0.63	This work	
	8.8	4	4.3	2.4	0.59	Exp	[33]
	10.3	3.2	4.5	3.55	0.46	XHTB	[34]
	8.9	3.8	3.7	2.55	0.56	BOM	[33]
	11.7	6.4	2.6	2.65	0.66	DFT	[1]
	9.3	3.9	4.6	2.7	0.56	PW-PP	[9]
InN	21.4	9.4	11	6	0.57	This work	
	20.4	11.6	17.7	4.4	0.68	PW-PP	[9]
	18.5	10.7	8	3.9	0.69	DFT	[1]
	17.2	11.9	3.7	2.65	0.78	LSF	[37]
	18.7	12.5	8.6	3.1	0.76	Ab initio	[32]
InP	10.2	5	4.9	2.6	0.62	This work	
	10.2	5.8	4.6	2.2	0.68	Exp	[9]
	11	5.6	5.3	2.7	0.63	PW-PP	[9]
	9.5	4.4	3.8	2.55	0.59	XHTB	[34]
	9.5	4.1	3.8	2.7	0.57	BOM	[33]
InAs	9.1	4.6	4.3	2.25	0.63	This work	
	8.3	4.5	4	1.9	0.66	Exp	[34]
	9.2	4.7	4.4	2.25	0.63	PW-PP	[9]
	9.2	3.9	3.7	2.65	0.56	XHTB	[34]
	8.1	3.5	3.3	2.3	0.57	BOM	[33]

Table 7 (*continued*)

Solids	C_{11}	C_{12}	C_{44}	$(C_{11}-C_{12})/2$	ζ Eq. (32)	Method	Ref.
InSb	6.6	3.7	3	1.45	0.68	This work	
	6.7	3.7	3	1.5	0.67	Exp	[34]
	7.2	3.5	3.4	1.85	0.61	PW-PP	[9]
	7.8	2.7	3.4	2.55	0.49	XHTB	[34]
	5.9	2.5	2.4	1.7	0.56	BOM	[33]
BN	54.4	22.1	28.9	16.15	0.54	This work	
	82	19	48	31.5	0.38	Exp.	[33]
	52.8	25.5	20.2	13.65	0.61	XHTB	[34]
	121	50.5	48.5	35.25	0.55	BOM	[33]
	84.4	19	48.3	32.7	0.38	Ab initio	[33]
	81.8	18	47	31.9	0.37	PW-PP	[9]
	83.7	18.2	49.3	32.75	0.37	DFT	[1]
BP	25.8	11.1	13.4	7.35	0.57	This work	
	31.5	10	16	10.75	0.46	Exp.	[33]
	35.4	7	14.4	14.2	0.35	XHTB	[33]
	42.6	17.6	17.5	12.5	0.55	BOM	[33]
	35.9	8.1	20.2	13.9	0.38	Ab initio	[33]
	35.9	8.1	19.7	13.9	0.38	PW-PP	[9]
Bas	21.8	9.5	11.2	6.15	0.57	This work	
	27.4	7	12.3	10.2	0.41	XHTB	[34]
	29.1	7.3	15.8	10.9	0.40	PW-PP	[9]
BSb	16.4	7.5	8.3	4.45	0.59	This work	
	20.5	6.3	11.2	7.1	0.45	PW-PP	[9]
TiN	20.4	9	10.4	5.7	0.57	This work	
	19.4	11.5	10.3	3.95	0.70	PW-PP	[9]
TiP	11	5.4	5.4	2.8	0.62	This work	
	10.8	5.3	5.4	2.75	0.62	PW-PP	[9]
TiAs	9.6	4.8	4.6	2.4	0.63	This work	
	8.9	4.4	4.4	2.25	0.62	PW-PP	[9]
TiSb	7.3	3.9	3.3	1.7	0.65	This work	
	6.9	3.4	3.4	1.75	0.62	PW-PP	[9]
ZnS	10.8	6.4	5.2	2.2	0.70	This work	
	10.4	6.5	4.6	1.95	0.73	Exp	[34]
	9.3	6.4	2.5	1.45	0.78	XHTB	[34]
	12.1	5.7	4.7	3.2	0.60	BOM-TB	[28]
	12.4	6.2	6	3.1	0.63	FP-LMTO	[7]
	11.8	7.2	7.5	2.3	0.72	FP-APW-lo	[7]
ZnSe	8.8	5.5	4.2	1.65	0.73	This work	
	8.1	4.9	4.4	1.6	0.71	Exp	[34]
	8.7	5.4	2.6	1.65	0.72	XHTB	[34]
	9.1	5.6	3.8	1.75	0.72	DFT	[1]
	9.5	4.5	3.7	2.5	0.60	BOM-TB	[28]
	9.6	5.4	4.9	2.1	0.68	FP-LMTO	[7]
	9.4	6.1	6.4	1.65	0.75	FP-APW-lo	[7]
ZnTe	6.5	4.4	2.9	1.05	0.77	This work	
	7.1	4.1	3.1	1.5	0.69	Exp	[34]
	7.6	4	2.8	1.8	0.65	XHTB	[34]
	8.6	5.5	3.1	1.55	0.74	DFT	[1]
	9.8	3.2	2.3	3.3	0.47	BOM-TB	[28]
	8.2	4.2	5.5	2	0.64	FP-APW-lo	[7]
CdS	7.9	5.1	3.7	1.4	0.74	This work	
	6.6	4.7	1.6	0.95	0.79	XHTB	[34]
			2.8	1.8		BOM-TB	[28]
CdSe	6.7	4.5	3	1.1	0.76	This work	
CdTe	4.8	3.6	2	0.6	0.82	This work	
	5.4	3.7	2	0.85	0.77	Exp	[34]
	5.7	3.2	1.9	1.25	0.68	XHTB	[34]
			1.3	0.9		BOM-TB	[28]
HgS	7.8	5	3.6	1.4	0.74	This work	
HgSe	6.6	4.4	3	1.1	0.76	This work	
HgTe	4.8	3.6	2	0.6	0.82	This work	

Table 7 (*continued*)

Solids	C_{11}	C_{12}	C_{44}	$(C_{11}-C_{12})/2$	ζ Eq. (32)	Method	Ref.
BeS	16.3	8.9	8.2	3.7	0.66	This work	
	16.5	9.8	5.4	3.35	0.70	XHTB	[34]
			16.4	11.5		BOM-TB	[28]
BeSe	13.7	7.7	6.8	3	0.68	This work	
	15.2	8.1	5.5	3.55	0.65	XHTB	[34]
			13.1	9.2		BOM-TB	[28]
BeTe	9.7	5.9	4.7	1.9	0.71	This work	
	12.7	5.4	5.2	3.65	0.56	XHTB	[34]
			8.2	5.8		BOM-TB	[28]

[LSF](Least Sqaure Fit).

Table 8
Values of the elastic stiffness constant (C_{44} in 10^{11} ergs/cm^3), Bulk modulus (B in 10^{11} ergs/cm^3), Shear modulus (G in 10^{11} ergs/cm^3) and Young's modulus (Y in 10^{11} ergs/cm^3) defined by Eqs. (16), (29)–(31) respectively obtained for zinc blende solids.

Solids	C_{44}	B	Y	G	Method	Ref.
AlN	12.6	18.93	23.08	13.22	This work	
	10.7	20.33	18.72	14.78	PW-PP	9
	13.3	20.20	24.53	11.76	LSF	37
	13.3	22.80	23.86	11.7	Ab initio	31
	10.4	20.87	18.16	13.9	DFT	1
		20.1		11.5	Exp	2
AlP	5.3	8.73	9.61	5.54	This work	
	5.0	8.90	8.81	5.1	PW-PP	9
	5.2	8.03	9.51	4.58	XHTB	34
	5.0	9.00	8.82	5.52	DFT	1
		8.6			Exp	2
AlAs	4.7	7.90	8.34	4.86	This work	
	4.6	7.87	8.22	4.66	Exp	33
	5.2	7.40	9.62	4.56	XHTB	34
	5.2	7.97	9.61	4.6	BOM	34
	4.5	7.53	8.06	4.64	Ab initio	33
	4.3	7.50	7.59	4.44	PW-PP	9
		7.7			Exp	2
AlSb	3.1	5.73	5.38	3.2	This work	
	3.4	5.90	5.99	3.42	Exp	9
	4.3	5.40	8.22	3.9	XHTB	34
	3.7	5.67	6.88	3.28	BOM	33
	3.3	5.60	5.95	3.3	PW-PP	9
		5.9		3.1	Exp	2
GaN	12.3	18.60	22.58	12.96	This work	
	12.2	20.70	21.85	15.18	PW-PP	9
	9.7	20.23	16.88	11.42	DFT	1
	10.4	20.37	18.11	11.98	Ab initio	32
	8.8	19.00	15.17	6.3	LSF	37
		19.0			Exp	2
GaP	5.3	8.73	9.61	5.54	This work	
	5.6	8.90	10.21	5.82	Exp	9
	5.6	8.17	10.32	4.96	XHTB	34
	5.9	8.97	10.79	5.2	BOM	33
	6.0	8.97	11.12	6.46	Ab initio	33
	6.2	9.23	11.39	6.32	PW-PP	9
	6.0	8.97	11.12	6.46	DFT	1
		8.88		5.8	Exp	2
GaAs	4.5	7.63	8.07	4.7	This work	
	4.7	7.47	8.51	4.84	Exp	1
	5.3	7.23	10.03	4.76	XHTB	34
	5.1	7.70	9.34	4.5	BOM	33

Table 8 (*continued*)

Solids	C_{44}	B	Y	G	Method	Ref.
	5.0	7.63	9.11	5.12	Ab initio	33
	5.1	7.53	9.43	5.24	PW-PP	9
	4.8	7.70	8.66	5.34	DFT	1
		7.56		4.88	Exp	2
GaSb	3.2	5.80	5.62	3.24	This work	
	3.5	5.60	6.30	3.54	Exp	33
	4.5	5.57	8.78	4.12	XHTB	34
	3.6	5.50	6.63	3.24	BOM	33
	4.1	8.17	7.17	2.62	DFT	1
	3.8	5.70	7.00	3.84	PW-PP	9
		5.74		3.54	Exp	2
InN	8.6	13.40	15.66	9	This work	
	6.9	14.53	11.99	12.38	PW-PP	9
	6.2	13.30	10.66	6.36	DFT	1
	4.5	13.67	7.47	3.28	LSF	37
	5.2	14.57	8.68	6.4	Ab initio	32
		13.7			Exp	2
InP	3.9	6.73	6.91	3.98	This work	
	3.5	7.27	6.00	3.64	Exp	9
	4.1	7.40	7.22	4.26	PW-PP	9
	3.7	6.10	6.71	3.3	XHTB	34
	3.8	5.90	7.03	3.36	BOM	33
		7.25		3.65	Exp	2
InAs	3.4	6.10	6.01	3.48	This work	
	2.9	5.77	5.14	3.16	Exp	34
	3.4	6.20	6.02	3.54	PW-PP	9
	3.7	5.67	6.88	3.28	XHTB	34
	3.3	5.03	5.99	2.9	BOM	33
		6.0		3.14	Exp	2
InSb	2.3	4.67	3.94	2.38	This work	
	2.3	4.70	4.07	2.4	Exp	34
	2.7	4.73	4.91	2.78	PW-PP	9
	3.4	4.40	6.41	3.06	XHTB	34
	2.4	3.63	4.41	2.12	BOM	33
		4.67		2.42	Exp	2
BN	22.5	32.87	41.63	23.8	This work	
	37.1	40.00	74.85	41.4	Exp.	33
	20.2	34.60	36.19	17.58	XHTB	34
	49.5	74.00	91.26	43.2	BOM	33
	38.2	40.80	77.42	42.06	Ab initio	33
	37.0	39.27	75.31	40.96	PW-PP	9
	37.9	40.03	77.20	42.68	DFT	1
		36.9		41.4	Exp	2
BP	10.4	16.00	19.12	10.98	This work	
	13.8	17.17	26.68	13.9	Exp.	33
	16.1	16.47	33.09	14.32	XHTB	33
	17.5	25.93	32.31	15.5	BOM	33
	16.2	17.37	32.92	17.68	Ab initio	33
	16.2	17.37	32.92	17.38	PW-PP	33
		17.3		13.9	Exp	2
Bas	8.8	13.60	16.03	9.18	This work	
	12.3	13.80	24.55	11.46	XHTB	34
	13.1	14.57	26.17	13.84	PW-PP	9
BSb	6.5	10.47	11.69	6.76	This work	
	9.0	11.03	17.54	9.56	PW-PP	9
TiN	8.2	12.80	14.89	8.52	This work	
	6.3	14.13	10.84	7.76	PW-PP	9
TiP	4.2	7.27	7.44	4.36	This work	
	4.1	7.13	7.31	4.34	PW-PP	9
TiAs	3.6	6.40	6.40	3.72	This work	
	3.4	5.90	5.99	3.54	PW-PP	9
TiSb	2.6	5.03	4.58	2.66	This work	
	2.6	4.57	4.66	2.74	PW-PP	9

Table 8 (*continued*)

Solids	C_{44}	B	Y	G	Method	Ref.
ZnS	3.5	7.87	6.04	4	This work	
	3.2	7.80	5.40	3.54	Exp	34
	2.5	7.37	4.08	2.08	XHTB	34
	4.7	7.83	8.45	4.1	BOM-TB	28
	4.7	8.27	8.27	4.84	FP-LMTO	7
	3.7	8.73	6.34	5.42	FP-APW-lo	7
		8.41		3.19	Exp	2
ZnSe	2.7	6.60	4.57	3.18	This work	
	2.6	5.97	4.41	3.28	Exp	34
	2.7	6.50	4.56	2.22	XHTB	34
	2.8	6.77	4.83	2.98	DFT	1
	3.7	6.17	6.61	3.22	BOM-TB	28
	3.3	6.80	5.71	3.78	FP-LMTO	7
	2.7	7.20	4.60	4.5	FP-APW-lo	7
		6.24		3.29	Exp	2
ZnTe	1.8	5.10	2.95	2.16	This work	
	2.4	5.10	4.10	2.46	Exp	34
	2.8	5.20	4.84	2.4	XHTB	34
	2.6	6.53	4.31	2.48	DFT	1
	4.3	5.40	8.22	2.7	BOM-TB	28
	3.0	5.53	5.35	4.1	FP-APW-lo	7
		5.1		2.48	Exp	2
CdS	2.3	6.03	3.90	2.78	This work	
	1.6	5.33	2.69	1.34	XHTB	34
		6.48		1.69	Exp	2
CdSe	1.9	5.23	3.08	2.24	This work	
		5.57		1.36	Exp	2
CdTe	1.1	4.00	1.71	1.44	This work	
	1.4	4.27	2.39	1.54	Exp	34
	2.0	4.03	3.40	1.64	XHTB	34
		4.24		1.05	Exp	2
HgS	2.3	5.93	3.89	2.72	This work	
HgSe	1.8	5.13	3.08	2.24	This work	
		4.85		1.65	Exp	2
HgTe	1.1	4.00	1.71	1.44	This work	
		4.37		1.29	Exp	2
BeS	5.7	11.37	10.01	6.4	This work	
	5.4	12.03	9.20	4.58	XHTB	34
BeSe	4.7	9.70	8.16	5.28	This work	
	5.5	10.47	9.57	4.72	XHTB	34
BeTe	3.1	7.17	5.24	3.58	This work	
	5.2	7.83	9.48	4.58	XHTB	34

[LSF](Least Sqaure Fit).

constants (C_{ij}) and may be represented by linear equations. These are simple function of product of ionic charges of cation and anion (Z_1Z_2) and nearest neighbour distance (d in Å); for zinc blende-structure semiconductors and compared their values with other theoretical calculations and experiments. Predictions of the hybrid covalent energy (V_2) for semiconductors are given in Table 2 together with the Bond orbital method (BOM) and Extended Huckel Tight Binding (XHTB) values [13]. Results for the polarity (α_p) obtained from linear equation (27) are listed in Table 3, together with those for the the Bond Orbital Method (BOM), Huckel Tight Binding (HTB), Extended Huckel Tight Binding (XHTB), Phillips (Ph), the cluster method (cl), Brillouin zone (BZ) integration of the LCAO Hamiltonian [28].

For comparison, the values of polarity ($\alpha_p \cong f_i$) given by Phillips (Ph) [13] and obtained by experiment (from the experiment-deduced ionicity scale (the definition is the same as Harrison's polarity) of Falter et al. [30]), are also given in Table 3. From a comparison of these values, we see that results obtained from linear equation (27) are in good agreement with the experiments. The value of the hybrid covalency (α_c), effective atomic charge (Z_{eff}) and transverse charge (e_T) has been calculated by Eqs. (9b), (9c) and (9d) correspondingly. The experimental values for effective atomic charge (Z_{eff}) and transverse charge (e_T) are also listed for comparison from Ref. [28]. It is clear from Tables 4 and 5 that the effective atomic charge (Z_{eff}) and transverse charge (e_T) are in good agreement with the experiments in most cases from the calculation of ETB; the

Table 9
Values of the bond stretching force constant (α in N/m), and bond bending force constant (β in N/m) defined by Eqs. (19) and (20) respectively obtained for zinc blende solids.

Solids	β [17]	β [35,36]	β [19]	β (This work)	α [17]	α [35,36]	α [19]	α (This work)
BN				29.26				109.42
BP	14.48		15.60	16.77	75.21		87.14	67.12
Bas	12.74		13.42	14.65	66.94		74.95	60.09
BSb			10.14	11.63			56.61	50.16
TiN			12.13	13.88			67.73	57.54
TiP			7.38	8.14			41.21	38.93
TiAs			6.63	7.10			37.05	35.63
TiSb			5.48	5.35			30.59	30.19
AlN	15.87		17.42	19.20	81.68		97.30	75.26
AlP	9.07		8.67	9.84	48.78		48.41	44.35
AlAs	8.15		7.94	8.89	44.10		44.34	41.33
AlSb	6.15	6.63	6.05	6.24	33.77	35.74	33.81	32.95
GaN	14.77		17.15	18.94	76.60		95.76	74.39
GaP	8.91	10.40	8.67	9.84	48.00	48.57	48.41	44.35
GaAs	7.74	8.88	7.75	8.64	42.04	43.34	43.27	40.51
GaSb	5.84	7.16	6.12	6.34	32.08	34.42	34.19	33.27
InN	11.35		12.66	14.45	60.14		70.70	59.44
InP	7.15	6.26	6.95	7.55	39.02	44.29	38.83	37.06
InAs	6.49	5.47	6.41	6.77	28.88	30.44	35.79	34.59
InSb	5.23	4.73	5.14	4.79	28.88	30.44	28.68	28.48
ZnS	4.54	4.36	4.46	5.97	49.09	44.73	42.22	40.38
ZnSe	4.05	4.65	3.84	4.76	44.26	38.61	36.34	35.69
ZnTe	3.52	4.47	3.11	3.19	39.02	32.04	29.40	29.76
CdS	3.58		3.57	4.20	39.63		33.81	33.58
CdSe	3.14		3.18	3.35	35.22		30.08	30.36
CdTe	2.71	2.48	2.58	1.92	30.65	29.44	24.38	25.09
HgS	4.18		3.53	4.12	39.47		33.41	33.25
HgSe	3.13	2.37	3.14	3.27	30.12	37.43	29.74	30.06
HgTe	2.34	2.54	2.61	1.99	22.79	29.32	24.65	25.35
BeS				8.91				52.10
BeSe				7.59				46.77
BeTe				5.34				37.95

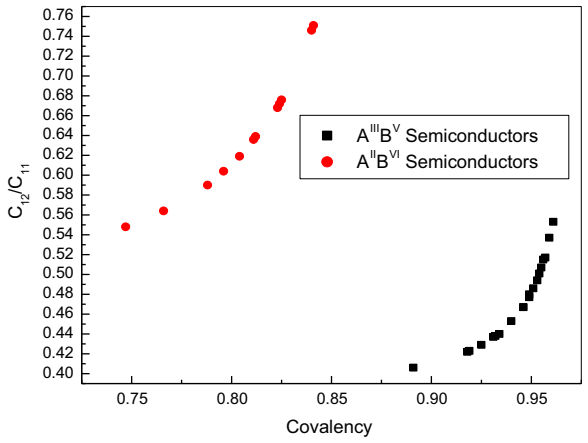

Fig. 7. Curve for the ratio C_{12}/C_{11} as a function of covalency (α_c).

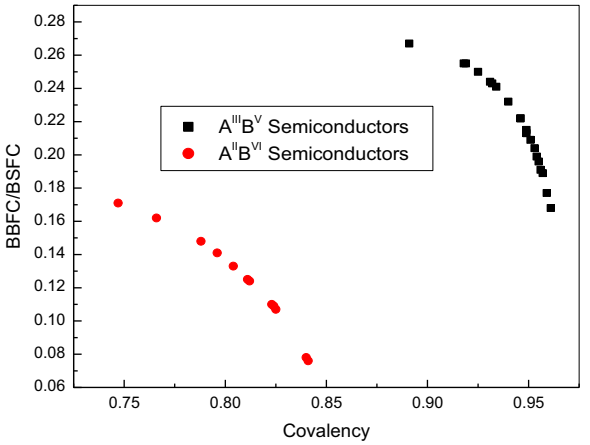

Fig. 8. Curve for the ratio β/α of bond bending force constant (BBFC=β) to bond stretching force constant (BSFC=α) as a function of covalency (α_c).

transverse charges are about one electron less than in the experiments in Ref. [28] from the calculation of BOM. When the experimental value of polarity (α_p) is used in [28], one cannot obtain the transverse charges, which are comparable with experiments. It is remarkable that the values of transverse charge (e_T) has shown good agreement with experimental values by ETB. It is remarkable that the values of hybrid covalent energy (V_2) has shown good agreement for the calculation of bulk modulus ($B=\lambda V_2/d^3$) in Table 6 from Eq. (24), with an accuracy of the order of a few per cent for most cases.

The results for the elastic constants (C_{11}, C_{12} and C_{44}) obtained from Eq. (28) are shown in Table 7 together with calculated values of Kleinman's internal displacement parameter from Eq. (32). Comparison of elastic stiffness constants (C_{44}), bulk modulus (B), Young's modulus (Y)

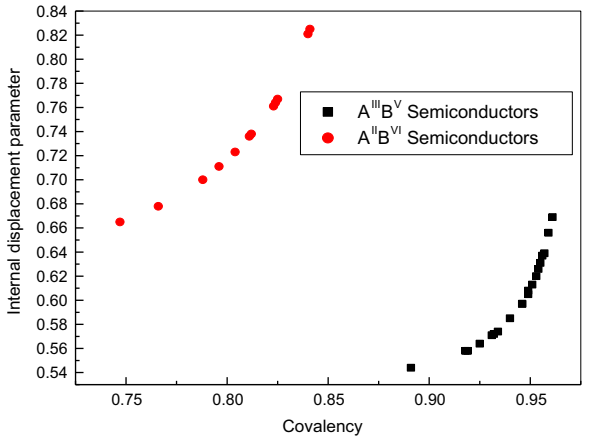

Fig. 9. Curve for the Kleinman's internal displacement parameters (ζ) versus covalency (α_c).

and shear modulus (G) obtained from ETB calculations with the experimental and other theoretical calculation results are shown in Table 8. The bond-stretching force constant (α) and bond-bending force constant (β) obtained from ETB calculations (neglecting the Coulomb contribution) with the theoretical quantities α and β derived from the calculated values of B and $(C_{11}-C_{12})/2$ are also given in Table 9. Table 8 indicates that the results obtained by using the ETB are in good agreement with the experimental and other theoretical results. The ratios C_{12}/C_{11} and β/α are also given in Figs. 7 and 8. It is clear from the figures that, according to our calculations, the Kleinman's internal displacement parameter (ζ) and the ratio C_{12}/C_{11} monotonically decrease, while the ratios β/α monotonically increase with increase in covalency. The results versus covalency are shown in Figs. 7–9. The trend of ζ as a function of α_c, is shown in Fig. 9; it is similar to that given by Martin [27], Harrison [5] and Kitamura and Harrison [4]. The trends of C_{12}/C_{11} versus covalency α_c, are shown in Fig. 7, which are similar to that given by Kitamura et al. [13]. Falter et al. [30] have given the ratio of the non-central (bond-bending) force constant β to the central (bond-stretching) force constant α as a function of polarity. This ratio is a measure of the importance of the covalent bond in stabilizing the tetrahedral structure. In Fig. 8, we give a plot of β/α as a function of covalency (α_c). The trend is similar to that given by Falter et al. [30].

6. Summary and conclusion

We see that Extant Tight Binding (ETB) theory makes it possible to estimate most of the properties of covalent solids; values are available for all of the needed parameters. The estimates become simple if we take an appropriate outlook, and that outlook is different for different systems. Extant Tight-Binding (ETB) calculations are simple, fast and more accurate; in regards of the applications point of view it can be highly dependent. The only information needed for calculating physical properties of covalent semiconductors by proposed relations is the nearest neighbour distance and ionic charge. We come to the conclusion that product of ionic charge of any compound is key parameter for calculating physical properties. It is also noteworthy that the proposed relations are simpler widely applicable and values are in better agreement with experiment data as compared to the relations proposed by previous researchers. Since, we have been reasonably successful in calculating these parameters using the product of ionic charge of the materials for binary crystals. It is natural to say that this model can easily be extended to ternary crystals for which the work is in progress and will be appearing in forthcoming paper. The method presented in this work will be helpful to the material scientists for finding new materials with desired physical properties among series of structurally similar materials.

References

[1] B. Derby, Phys. Rev. B 76 (2007) 054126.
[2] S. Kamran, K. Chen, L. Chen, Phys. Rev. B 77 (2008) 094109.
[3] S.Q. Wang, H.Q. Ye, Phys. Rev. B 66 (2002) 235111.
[4] M. Kitamura, W.A. Harrison, Phys. Rev. B 44 (1991) 7941.
[5] W.A. Harrison, Electronic Structure and the Properties of Solids, Freeman, New York, 1980.
[6] B.N. Harmon, W. Weber, D.R. Hamann, Phys. Rev. B 25 (1982) 1109.
[7] R. Khenata, A. Bauhemadou, M. Sahnoun, A.H. Reshak, H. Baltache, M. Rabah, Comput. Mater. Sci. 38 (2006) 29.
[8] H.M. Tutuncu, S. Wagci, G.P. Srivastava, A.T. Albudak, G. Ugur, Phys. Rev. B 71 (2005) 195309.
[9] S.Q. Wang, H.Q. Ye, Phys. Status Solidi B 240 (2003) 45.
[10] S.Q. Wang, H.Q. Ye, J. Phys.: Condens. Matter 14 (2002) 9579.
[11] M. Methfessel, C.O. Rodriguez, O.K. Anderson, Phys. Rev. B 40 (1989) 2009.
[12] F. Bechstedt, W.A. Harrison, Phys. Rev. B 39 (1989) 5041.
[13] M. Kitamura, S. Muramatsu, W.A. Harrison, Phys. Rev. B 46 (1992) 1351.
[14] A.S. Verma, Phys. Scr. 79 (2009) 045703.
[15] A.S. Verma, Phys. Lett. A. 372 (2008) 7196.
[16] L. Pauling, in: Bond 3rd (Ed.), The Nature of the Chemical, Cornell University Press, Ithaca, 1960.
[17] V. Kumar, J. Phys. Chem. Solids 61 (2000) 91.
[18] A.S. Verma, Mater. Chem. Phys. 139 (2013) 256.
[19] A.S. Verma, Solid State Commun. 158 (2013) 34.
[20] A.S. Verma, Solid State Commun. 149 (2009) 1236.
[21] A.S. Verma, Phys. Status Solidi B 246 (2009) 192.
[22] A.S. Verma, Phys. Status Solidi B 246 (2009) 345.
[23] A.S. Verma, Philos. Mag. 89 (2009) 183.
[24] W.A. Harrison, Phys. Rev. B 23 (1981) 5230.
[25] R.G. Gordon, Y.S. Kim, J. Chem. Phys. 56 (1972) 3122.
[26] J.M. Baranowski, J. Phys. C: Solid State Phys. 17 (1984) 6287.
[27] R.M. Martin, Phys. Rev. B 1 (1970) 4005.
[28] S.G. Shen, J. Phys.: Condens. Matter 6 (1994) 8733.
[29] N. Bouarissa, M. Boucenna, Phys. Scr. 79 (2009) 15701.
[30] C. Falter, W. Ludwing, M. Selmke, W. Zierau, Phys. Lett. 105A (1984) 139.
[31] E. Ruiz, S. Alvarez, P. Alemany, Phys. Rev. B 49 (1994) 7115.
[32] A.F. Wright, J. Appl. Phys. 82 (1997) 2833.
[33] T. Azuhata, T. Sota, K. Suzuki, J. Phys: Condens. Matter 8 (1996) 3111.
[34] S. Muramatsu, M. Kitamura, J. Appl. Phys. 73 (1993) 4270.
[35] H. Neumann, Cryst. Res. Technol. 20 (1985) 773.
[36] H. Neumann, Cryst. Res. Technol. 24 (1989) 325.
[37] M.E. Sherwin, T.J. Drummond, J. Appl. Phys. 69 (1991) 8423.